

A new artificial photosynthetic system coupling photovoltaic electrocatalysis with photothermal catalysis

Yaguang Li^{1,4,*}, Fanqi Meng^{2,4}, Xianhua Bai^{1,4}, Dachao Yuan³, Xingyuan San¹, Baolai Liang¹, Guangsheng Fu¹, Shufang Wang¹, Lin Gu², Qingbo Meng^{2,*}

¹Hebei Key Lab of Optic-electronic Information and Materials, The College of Physics Science and Technology, Institute of Life Science and Green Development, Hebei University, Baoding, 071002, China.

²Beijing National Laboratory for Condensed Matter Physics, Institute of Physics, Chinese Academy of Sciences, Beijing, 100190, China.

³College of Mechanical and Electrical Engineering, Hebei Agricultural University, Baoding 071001, China.

⁴These authors contributed equally to this work.

Correspondence and requests for materials should be addressed to Y. Li. (email: liyaguang@hbu.edu.cn) or to Q. Meng. (email: qbmeng@iphy.ac.cn).

Abstract

In this work, we present a novel artificial photosynthetic paradigm with square meter (m^2) level scalable production by integrating photovoltaic electrolytic water splitting device and solar heating CO_2 hydrogenation device, successfully achieving the synergy of 1 sun driven 19.4% solar to chemical energy efficiency (STC) for CO production (2.7 times higher than state of the art of large-sized artificial photosynthetic systems) with a low cost (equivalent to 1/7 of reported artificial photosynthetic systems). Furthermore, the outdoor artificial photosynthetic demonstration with 1.268 m^2 of scale exhibits the CO generation amount of 258.4 L per day, the STC of $\sim 15.5\%$ for CO production in winter, which could recover the cost within 833 sunny days of operation by selling CO.

Introduction

Artificial photosynthesis can convert CO_2 and H_2O into useful fuels, chemicals (CO ,¹ CH_4 ,² etc.) and O_2 under solar irradiation, which is the most important way for carbon neutralization.³⁻⁹ The application of large-scale artificial photosynthesis is of great significance to weaken the global warming, overcome the current energy and environmental crisis.¹⁰⁻¹² More recently, several large-sized artificial photosynthetic systems for CO_2 utilization have been reported, e. g., the solar fuel production chain with square meters (m^2) scale,¹³ the photovoltaic electrocatalytic device with $\sim 0.1 \text{ m}^2$ scale.¹⁴ To the best of our knowledge, the highest solar to chemical energy efficiency

(STC) of large-sized devices is 7.2% by the photovoltaic electrocatalytic system.¹⁴ However, the material cost for constructing large-sized artificial photosynthetic system is too expensive to practical application, due to the using of noble metal catalysts (e.g., Ir, Pt, Rh, Ru) and the costliness of large-sized components (e.g., membranes, solar reactor) in the devices.^{15,16} Therefore, it is one of the holy grails of the entire scientific and technological community to achieve a scalable artificial photosynthetic system with high STC and low cost simultaneously, so as to realize the sustainable development of human society.

Herein, we have developed a new artificial photosynthetic system by integrating a photovoltaic electrolytic H₂O decomposition part and a solar heating CO₂ hydrogenation part. Just relying on such a simple strategy, this system not only changed the reaction path and mass transportation but also discarded all rare elements and expensive components, resulting in the m² level scalable production and a record STC (19.4%) with low cost. Moreover, an outdoor demonstration (1.268 m² scale) of this new design was built based on full commercial components and the STC was still higher than 15% at outdoor test in winter. This artificial photosynthetic system could recover the total system cost within 833 days of operation by selling the products of CO.

Conception for constructing novel artificial photosynthetic system

It is well known that the widely studied photovoltaic electrocatalytic systems contain the competition of two main reactions: H₂O decomposition and CO₂ hydrogenation on one system with CO₂ transportation through liquid electrolytes. Although various

efficient catalysts have been developed, such as metals,¹⁷⁻¹⁹ metal compounds,²⁰⁻²² molecular complexes,^{23,24} photovoltaic electrocatalysis still faces two intrinsic shortcomings: one is the complex reaction processes in single catalytic system and the other is the sluggish CO₂ supply through gas/liquid transportation.²⁵⁻²⁷ Here, a new paradigm of artificial photosynthesis is proposed to separate the two reactions of water splitting ($2\text{H}_2\text{O} \rightarrow 2\text{H}_2 + \text{O}_2$)²⁸ and CO₂ hydrogenation ($\text{CO}_2 + \text{H}_2 \rightarrow \text{CO} + \text{H}_2\text{O}$)²⁹⁻³¹ in space and time. There are four major advantages in this new system: (1) mature technologies can be selected for both water splitting and CO₂ hydrogenation; (2) the integrated system can be easily enlarged; (3) the systems for the two reactions can be optimized separately, providing a variety of possibilities for efficiency, cost and products; (4) CO₂ supply can be boosted by avoiding the gas transport in liquid electrolytes. As shown in Fig.1, this is an integrated system in which the hydrogen generated from photovoltaic water electrolysis³² is directly injected into the solar heating system for CO₂ hydrogenation.³³⁻³⁵ The CO₂ transportation of this system is in gas diffusion mode at a rate of $10^{-5} \text{ m}^2 \text{ s}^{-1}$,³⁶ 10000 times higher than the rate of CO₂ diffused through liquid electrolytes ($10^{-9} \text{ m}^2 \text{ s}^{-1}$)³⁷ in conventional photovoltaic electrocatalytic systems,^{38,39} which could meet the CO₂ supply for large-sized artificial photosynthetic systems. For integrating such a new artificial photosynthetic system, the two issues should be solved firstly. One is the matching problem of solar energy utilization in this system, that is, how to scientifically distribute the proportion of solar energy irradiated to the two devices to improve the STC; the second is the quality matching of hydrogen production and hydrogen consumption in the new system.

Integrating the artificial photosynthetic system

A TiC/Cu heterostructure photothermal material was chosen to construct the solar heating catalytic system (Supplementary Fig. 1),⁴⁰⁻⁴² which could heat the catalysts to 318 °C under 1 kW m⁻² intensity of sunlight (1 sun) irradiation to run CO₂ hydrogenation (Supplementary Fig. 2). This is the key for realizing the new artificial photosynthetic system, because the low solar irradiated temperature of conventional photothermal system (~80 °C, Supplementary Fig. 3) can not drive photothermal CO₂ hydrogenation under ambient solar irradiation. As the Fe single-atom catalysts (Fe SACs, Supplementary Fig. 4-8) were used as catalysts for solar heating CO₂ hydrogenation, the system showed a CO generation rate of 21.14 mol m⁻² h⁻¹ under 1 sun irradiation, corresponding to 24.1% of solar to chemical energy efficiency (detailed calculation seen in Supplementary Methods, Supplementary Fig. 9). More interestingly, as the 1% O₂-polluted H₂ was used as feed gas, the efficiency of CO₂ hydrogenation had little change (Supplementary Fig. 9a) and this solar heating system still showed a straight forward CO production rate of ~21.1 mol m⁻² h⁻¹ more than 60 days (Supplementary Fig. 10), evidencing the robustness of solar heating catalytic system.

The low requirement of hydrogen purity for solar heating catalysis enables us to simplify the photovoltaic electrocatalysis. Besides using commercialized single crystalline silicon solar cells (23.5% efficiency) as electric energy supply, the membrane was eliminated from the electrocatalytic reactor (Fig. 1) and the cheap nickel-plated stainless-steel mesh (Ni/stainless steel, Supplementary Fig. 11) was used as the electrodes to replace the precious electrocatalysts.¹⁷⁻¹⁹ In the membrane free

electrocatalytic reactor, the Ni/stainless steel's electrodes could achieve a current density of 10 mA cm^{-2} in 1 M KOH electrolyte at only 1.53 V (Supplementary Fig. 12). The H_2 production rate of this photovoltaic electrolytic system was $2.40 \text{ mol m}^{-2} \text{ h}^{-1}$ under 1 sun irradiation (Supplementary Fig. 13), equivalent to 19.04% solar to hydrogen chemical efficiency (detailed calculation seen in Supplementary Methods). It was calculated that the solar cell's electric energy to chemicals energy efficiency (EC) of this photovoltaic electrocatalytic water splitting system was 81% (detailed calculation seen in Methods). The released H_2 contained $\sim 0.8\%$ O_2 , which also meets the purity requirement of solar heating CO_2 hydrogenation.

Based on the above experimental results, the photovoltaic electrolytic water splitting device with 2800 cm^2 of solar irradiation area and solar heating CO_2 hydrogenation device with 240 cm^2 of solar irradiation area were integrated as a new type of artificial photosynthetic system with more than 3000 cm^2 of solar irradiation area in the laboratory (Fig. 1).

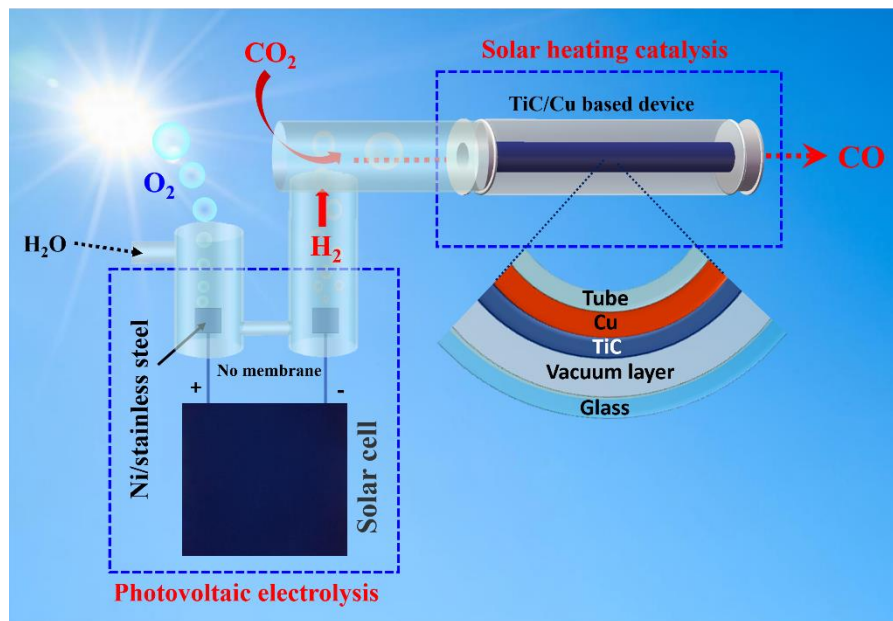


Fig. 1 Schematic map of the novel artificial photosynthesis.

The performance of novel artificial photosynthesis

Fig. 2a showed that the laboratory system could produce CO with a rate of 38, 210, 491 mmol h⁻¹ under 0.6, 0.8, 1 sun irradiation, respectively. Additionally, Fig. 2b identified that this system showed a 100% selectivity for CO₂ converted into CO under different intensities of solar irradiation due to the +3 oxidation state of Fe-SACs (Supplementary Fig. 14).⁴³ Fig. 2c illustrated that the STC of new artificial photosynthetic system was increased from 11.3%, 17.4% to 19.4% along with the 0.6, 0.8 to 1 sun irradiation (Detailed calculation seen in Methods), which was 2.7 times higher than the best record value of scalable artificial photosynthesis with ~1000 cm² of solar irradiation area (7.2%).¹⁴ The CO₂ reduction performance of this system was continuously tested for 6 days, and the CO production rate was stable maintained at ~500 mmol h⁻¹ (Fig. 2d), indicating the excellent stability of new artificial photosynthetic system.

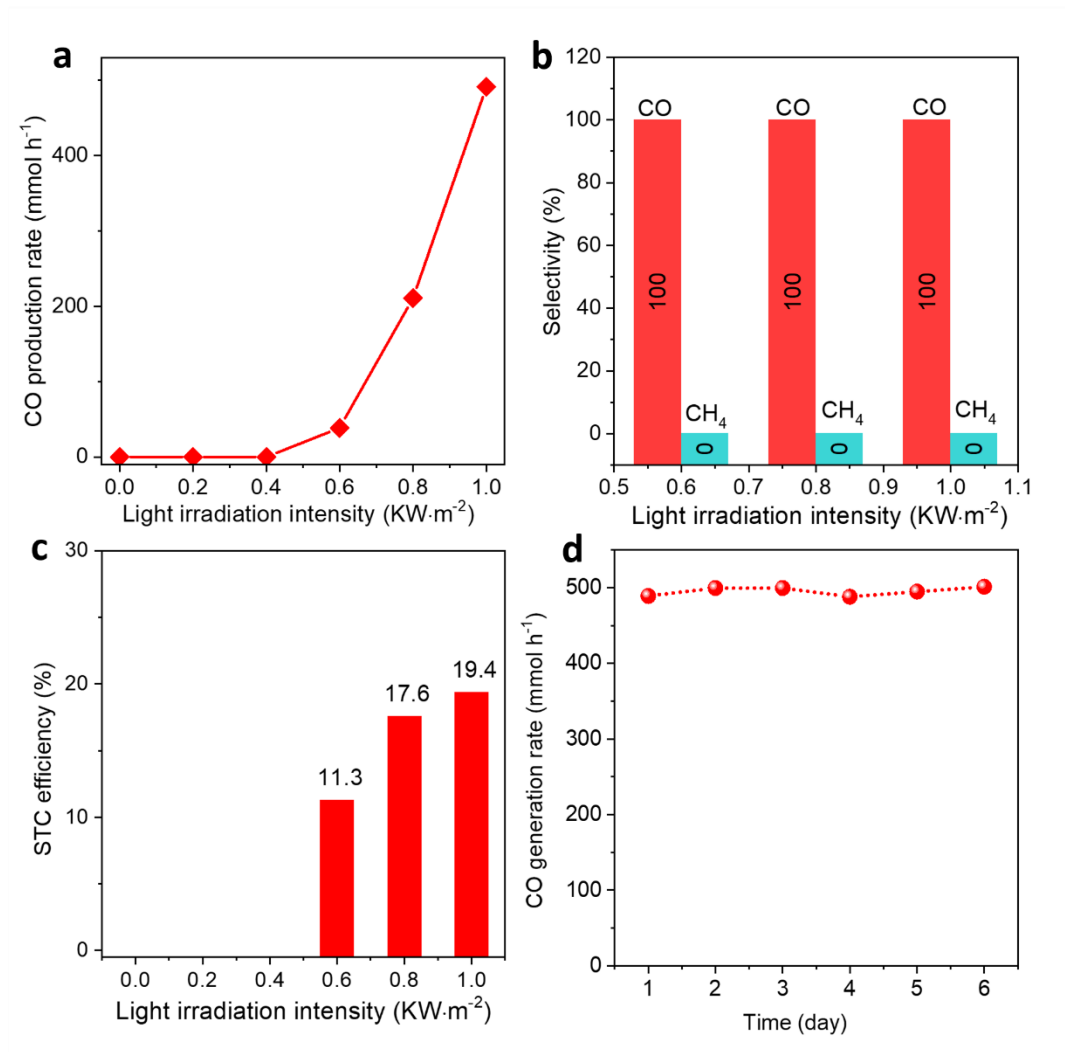


Fig. 2 The laboratory performance of novel artificial photosynthetic system. **a** The CO production rate of new artificial photosynthetic system with Fe SACs, under different intensities of solar irradiation. **b** The CO selectivity of new artificial photosynthetic system with Fe SACs, under different intensities of solar irradiation. **c** The STC efficiency of new artificial photosynthetic system with Fe SACs, under different intensities of solar irradiation. **d** The CO production rate stability of new artificial photosynthetic system under 1 sun irradiation.

The outdoor artificial photosynthetic demonstration

The commercial singlecrystalline silicon solar cell panel (1.07 m² scale), membrane-

free electrolytic water splitting device and factory prepared TiC/Cu based solar heating tube were used to build the outdoor artificial photosynthetic system. For maintaining the solar heating system at high temperature all day, a parabolic reflector with 0.198 m² of irradiated area (Supplementary Fig. 15) was applied to concentrate outdoor sunlight on solar heating device (Fig. 3a). A commercial CuO_x/ZnO/Al₂O₃ (SCST-401, Supplementary Fig. 16) was selected as the catalyst for solar heating reverse water-gas-shift reaction ($\text{CO}_2 + \text{H}_2 \rightarrow \text{CO} + \text{H}_2\text{O}$). In outdoor test, the membrane-free electrolytic water splitting device was driven by the silicon solar cell panel to produce H₂, then the H₂ and CO₂ entered into the solar heating system for CO₂ hydrogenation. The artificial photosynthetic system for CO production was tested in December 20, 2021, with an ambient temperature of 2~13 °C and a solar irradiation intensity of 0.26-0.49 kW m⁻² in the daytime in Baoding City of Hebei Province, China. As shown in Fig. 3c, the CO generation occurred at 9:00 AM with a production rate of 27.9 L h⁻¹. After that, the CO generation rate rose to a peak value of 41.4 L h⁻¹ at 12:00 PM and then gradually decreased to 23.6 L h⁻¹ at 16:00 PM. The total amount of CO produced daily was up to 258.4 L. Although the solar intensity and ambient temperature are the lowest in winter, the outdoor system STC for CO production was still in the range of 15% to 15.8% throughout the operating period (Fig. 3d, detailed calculation seen in Methods).

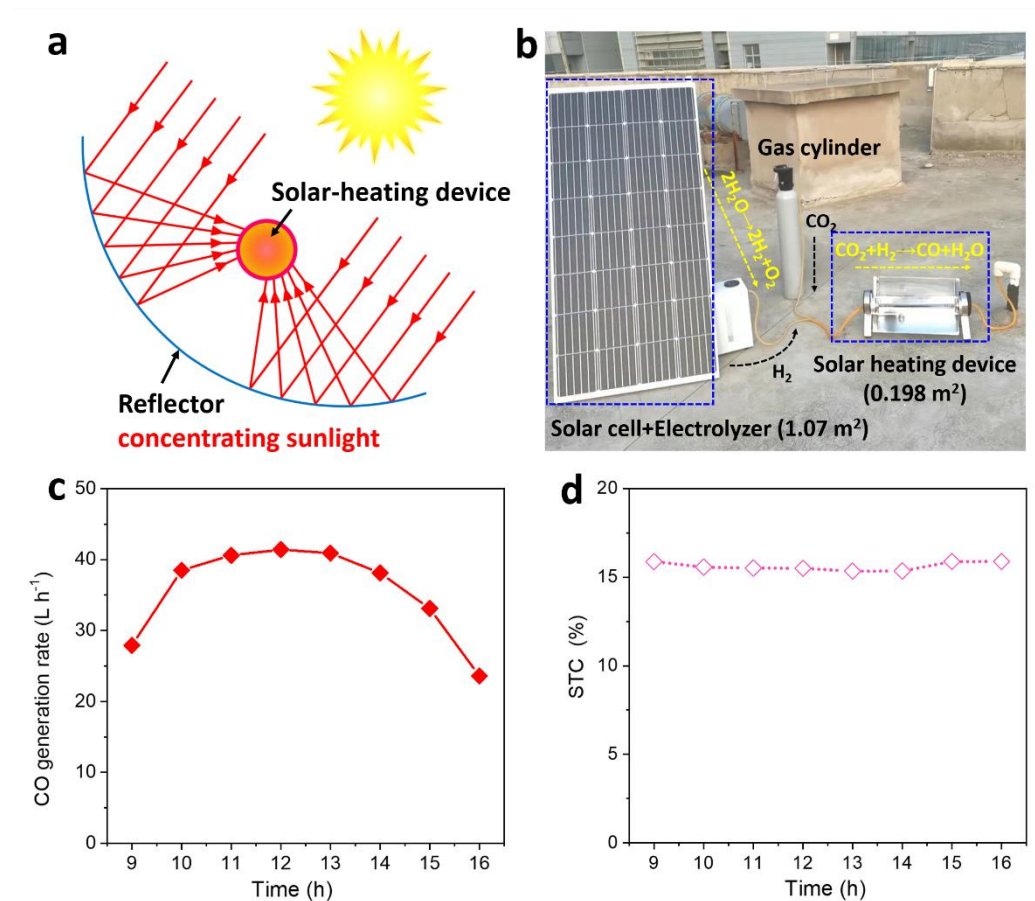


Fig. 3 The outdoor performance of novel artificial photosynthetic system. **a** The location diagram of reflector, solar heating device and solar. **b** The photograph of new artificial photosynthetic demonstration on the roof of the building in Hebei University. **c, d** The CO production rate and STC of new artificial photosynthetic demonstration under ambient sunlight irradiation, on December 20, 2021, in Baoding City, China.

Tab.1 listed the data of new artificial photosynthetic systems and the most advanced large-sized artificial photosynthetic systems. Firstly, the size of the outdoor artificial photosynthetic system was 1.268 m², and all parts can be processed in the factory, showing that the system could realize mass production directly. Secondly, the STCs of lab and outdoor systems for CO₂ reduction as CO were 19.4% and 15-15.8%

respectively, which was 2.7 times and 4 times higher than that of reported large-sized artificial photosynthetic systems under lab and outdoor conditions, respectively.^{13,14} The total cost of outdoor demonstration was calculated as \$1018 per m² (Supplementary Fig. 17). Tab. 1 showed that the cost of large-sized artificial photosynthetic devices is too expensive to calculated cost.^{13,14,44} As far as we known, the cheapest cost of small-sized artificial photosynthetic device reported in literatures was ~\$7200 per m² (Tab. 1),⁴⁵ which was 7 times higher than our outdoor demonstration. With the ultra-high STC and ultra-low system cost, the system cost recovery time of the outdoor artificial photosynthetic device was calculated by selling product (CO). Referring to the price of CO (\$6 per m³),⁴⁵ the outdoor system could recover the cost after 833 days of operation, which corresponds to ~3.5 years (detailed calculation seen in Methods). The service life of the components in this outdoor system for CO production was generally more than 10 years, able to profitable by selling CO.

Tab. 1 Comparison of the solar driven CO₂ reduction systems of this work and the state of the art of solar cells driven artificial photosynthetic systems. IA is the working solar illumination area of device used for CO₂ conversion.

Refs.	Condition	IA (cm ²)	Main product	STC (%)	Cost (\$ per m ²)
This work	outdoor	12,680	CO	15-15.8	1018
13	outdoor	65,000	CO+H ₂	3.8	None
44	outdoor	14,700	formic acid	1.86	None
This work	Lab	2,287	CO	19.4	None
45	Lab	14	CO	8.05	7200
14	Lab	987	formic acid	7.2	None
46	Lab	16	CO+H ₂	4.3	None

Conclusion

In this work, a novel artificial photosynthesis paradigm was proposed, in which the silicon solar cells were used to drive the membrane free electrolyzer for photovoltaic electrolytic water splitting as O₂ and H₂. Then, the generated H₂ and CO₂ were injected into the solar heating system based on a TiC/Cu based device to carry out efficient sunlight driven CO₂ hydrogenation due to the high 1 sun-heating temperature of 318 °C. The photovoltaic electrolytic reactor eliminated the membrane and used the Ni-plated stainless steel mesh as the electrodes to reduce the cost. As the 240 cm² of solar heating CO₂ hydrogenation device was integrated to 2800 cm² of silicon solar cell driven photovoltaic electrolytic water splitting device, the system exhibited a CO₂ conversion rate of 491 mmol h⁻¹, an STC of 19.4%, a selectivity of 100% for CO production, under 1 sun irradiation. Moreover, an outdoor demonstration with 1.268 m² of solar irradiation area was constructed, which showed a cost of \$1018 per m², the gas production of 258.4 L per day, the STC of 15%-15.8% for CO production in winter, under ambient solar irradiation, which could neutralize device cost by selling the product of CO within 833 sunny operation days, revealing the ability for direct scalable application.

Outlook

The new artificial photosynthetic system has huge space for STC improvement and flexible product regulated ability. As the silicon solar cell was replaced by triple-junction solar cells for photovoltaic electrocatalytic water splitting, the calculated STC

of new artificial photosynthetic system was as high as 28.9 % (detailed calculation seen in Supplementary Methods), which was higher than the best STC (19.1%) of triple-junction solar cells driven artificial photosynthesis.⁴⁷ Further, this system could convert product from CO to CH₄ by changing the solar heating CO₂ hydrogenation catalysts as commercial Ni/Al₂O₃ (Supplementary Fig. 18, detailed calculation seen in Methods). Therefore, this system could be a core platform for scientists all over the world to realize carbon neutralization via converting CO₂ and H₂O into a variety of chemicals.

Methods

Thermocatalytic CO₂ hydrogenation

The thermocatalytic activity of catalysts for CO₂ hydrogenation was tested by the fixed-bed reactor (XM190708-007, DALIAN ZHONGJIARUILIN LIQUID TECHNOLOGY CO., LTD) in continuous flow form. Typically, 10 mg of catalyst was placed in a quartz flow reactor. For CO production, the feed gas of CO₂/H₂/Ar = 1/1/48 or CO₂/99% H₂+1% O₂/Ar = 1/1/48 with 100 Sccm of flow rate was regulated by the mass flow controller. The reaction products were tested by gas chromatograph (GC) 7890A equipped with FID and TCD detectors.

Solar heating CO₂ hydrogenation as CO

The solar heating CO₂ hydrogenation was tested as follows: 137 g of Fe SACs were loaded into TiC/Cu based device (0.024 m²), and irradiated by a xenon lamp (ZSL-4000). In this test, CO₂ and 100% H₂ (or 99% H₂+1% O₂) with 1.5/1 ratio were mixed as feed gas. For the produced gas, the flow rate was tested by mass flowmeter and the

composition was tested by GC 7890A equipped with FID and TCD detectors. It was required to control the flow rate to make the H₂ consumption exceeds 95%. The data were collected by FID and TCD.

The CO rate (δ , mol m⁻² h⁻¹) was calculated as follows:

$$\delta \text{ (mol m}^{-2} \text{ h}^{-1}\text{)} = (L/(24.5*S)) \quad (1)$$

L was the CO flow rate (L h⁻¹). S was the irradiated area (0.024 m²). When using the 99% H₂+1% O₂ as feed gases, the L irradiated by 0.6, 0.8, 1 sun was 0.98, 5.32, 12.43 L h⁻¹, respectively.

Solar driven water splitting

The back contact silicon cells interdigitated with 2800 cm² irradiation area were purchased from SUNPOWER (23.5% efficiency) to drive an alkaline electrolyzer with 1 m² of Ni/Stainless steel mesh. Xenon lamp (HP-2-4000) was used as a light source and 1M KOH was used as the electrolyte for sunlight driven water splitting. The produced H₂ was injected into the TiC/Cu based device and the produced H₂ rate of the solar driven water splitting system was tested by mass flowmeter (C50 300SCCM).

The H₂ production rate for per m² (H , mol m⁻² h⁻¹) of solar cell was calculated as follows:

$$H \text{ (mol m}^{-2} \text{ h}^{-1}\text{)} = (\varepsilon/(24.5*S)) \quad (2)$$

ε (L h⁻¹) was the H₂ generation amount per hour detected by a flowmeter, S was the irradiated area (0.2800 m²). The ε irradiated by 0.4, 0.6, 0.8, 1 sun was 6.68, 10.02, 13.31, 16.45 L h⁻¹, respectively.

Enthalpy change energy of chemicals

The enthalpy change energy of CO₂ (g), CO (g), H₂ (g), O₂ (g), H₂O (g), H₂O (l) was -

393.505, -110.541, 0, 0, -241.818, -285.830 kJ mol⁻¹, respectively.

The (g) and (l) indicated the gas state and liquid state, respectively.

Novel artificial photosynthesis for CO₂ and H₂O converted as CO and O₂

As the solar driven water splitting produced H₂ injected into the TiC/Cu based device loaded with 137 g of Fe SACs, 600 sccm of CO₂ was simultaneously put into the TiC/Cu based device, which was controlled by mass flow controller (C50 5SLM). The TiC/Cu based device was irradiated by a xenon lamp (ZSL-4000). For the produced gas, the flow rate was tested by mass flowmeter (C50 5SLM) and the composition was tested by GC 7890A equipped with FID and TCD detectors.

The CO rate (δ , mmol h⁻¹) was calculated as follows:

$$\delta \text{ (mmol h}^{-1}\text{)} = (1000 * L / 24.5) \quad (3)$$

L was the CO flow rate (L h⁻¹) and the L irradiated by 0.6, 0.8, 1 sun was 0.946, 5.170, 12.030 L h⁻¹, respectively.

The STC calculation of sunlight driven CO₂ conversion as CO

The STC efficiency of novel artificial photosynthetic system for converting CO₂ into CO was calculated as follows:

$$\text{STC} = (\Delta H * \varepsilon) / (I * S * 3600) \quad (4)$$

ΔH was the reaction Enthalpy change energy (H₂O (l) + CO₂ (g) → CO (g) + 1/2 O₂ (g) + H₂O (g), $\Delta H = 326.9754$ kJ mol⁻¹), ε (mol) was the CO generation amount per hour detected by a flowmeter, I was the light intensity (kW m⁻²), S was the total irradiated area. The ε irradiated by 0.6, 0.8, 1 sun was 0.0386, 0.211, 0.491 mol, respectively.

Since not all H₂ produced from solar driven water splitting was used for CO₂

hydrogenation, the irradiation area (β) of solar driven water splitting used for CO₂ hydrogenation was calculated as follows:

$$\beta = M/N * 0.2800 \text{ m}^{-2} \quad (5)$$

The M was H₂ used for CO₂ hydrogenation as CO, which was equal to the CO production rate of 0.0386, 0.211, 0.491 mol h⁻¹, under 0.6, 0.8, 1 sun irradiation, respectively. The N was the H₂ production rate of 0.3931, 0.5273, 0.6714 mol h⁻¹, irradiated by 0.6, 0.8, 1 sun, respectively. Therefore, the β was 0.0276 m⁻², 0.1119 m⁻², 0.2047 m⁻², under 0.6, 0.8, 1 sun irradiation, respectively.

$$\text{And the } S = \beta + 0.0240 \text{ m}^{-2} \quad (6)$$

Therefore, the S was 0.0516, 0.1359, 0.2287 m⁻², under 0.6, 0.8, 1 sun irradiation, respectively.

Consequently, the STC was 11.3%, 17.6%, 19.4%, under 0.6, 0.8, 1 sun irradiation, respectively.

The EC calculation

The 1 sun driven EC of photovoltaic electrocatalytic water splitting in this work and reported photovoltaic electrocatalytic CO₂ reduction was calculated as follows:

$$\text{EC} = \text{STCE} / \text{efficiency} \quad (7)$$

The STCE was the solar to hydrogen chemical efficiency (19.04%) under 1 sun irradiation. The efficiency was the electric energy generation efficiency of solar cell (23.5%) under 1 sun irradiation. Therefore, the EC was calculated as 81.0%.

Outdoor artificial photosynthetic system

The outdoor artificial photosynthetic system consisted of two components. One

component was photovoltaic electrolysis system, in which the PERC solar cell (182DCB) with 1.07 m² of solar irradiation area was used to power electrolytic reactor with 2.782 m² of Ni/Stainless steel mesh divided into 12 independent chambers in series. The mixture of 200 g KOH and 1.8 L deionized water was used as the electrolyte. The other component was solar heating system, in which a solar heating device was provided by Hebei scientist research experimental and equipment trade Co., Ltd. with the size of 4 cm in diameter and 50 cm inlength, equipped with a reflector of 50 cm inlength and 36 cm in width. For the production of CO, the catalysts used in solar heater were 400 g CuO_x/ZnO/Al₂O₃. For CO production production in solar heating system, the CO₂/H₂ ratio was 1.5. It was required to control the flow rate to ensure the H₂ consumption exceeds 95%. The data were collected by FID and TCD. The data shown in Fig. 3c were tested on December 20, 2021, in Baoding, China.

The STC of outdoor artificial photosynthetic system

The STC of the outdoor artificial photosynthetic system for converting CO₂ into CO was calculated as follows:

$$STC = (\Delta H * \varepsilon) / (I * S * 3600 * 22.4) \quad (8)$$

ΔH was the reaction Enthalpy change energy ($H_2O(l) + CO_2(g) \rightarrow CO(g) + 1/2 O_2(g) + H_2O(g)$, $\Delta H = 326.9754 \text{ kJ mol}^{-1}$), ε (L) was the CO generation amount per hour detected by a flowmeter, I was the outdoor solar intensity (kW m^{-2}), S was the total irradiated area of 1.268 m².

The cost recovery calculation

We assumed that the CO production amount of the outdoor artificial photosynthetic

system was 258.4 L/day. Due to the variety of CO prices, the quotation of Chae et al. reported result⁴⁵ and North Special Gas Co., Ltd. was adopted, which was \$6 per m³ CO.

Therefore, the income of outdoor artificial photosynthetic system for CO production was 0.2584* \$6=\$1.55. To achieve an income of \$1291, this system required \$1291/\$1.55=833 sunny days, which were equivalent to the sunny days in 3.5 years, according to the weather in Baoding of 240 sunny days per year.

Data availability

The data that support the findings of this study are available from the corresponding authors upon reasonable requests.

References

- 1 Beck, A. *et al.* Following the structure of copper-zinc-alumina across the pressure gap in carbon dioxide hydrogenation. *Nat. Catal.* **4**, 488-497, (2021).
- 2 Zhou, B. *et al.* Highly efficient binary copper–iron catalyst for photoelectrochemical carbon dioxide reduction toward methane. *P. Nat. Acad. Sci.* **117**, 1330-1338, (2020).
- 3 Zhong, M. *et al.* Accelerated discovery of CO₂ electrocatalysts using active machine learning. *Nature* **581**, 178-183, (2020).
- 4 Wang, Y., Liu, J., Wang, Y., Wang, Y. & Zheng, G. Efficient solar-driven electrocatalytic CO₂ reduction in a redox-medium-assisted system. *Nat. Commun.* **9**, 5003, (2018).
- 5 Asadi, M. *et al.* Nanostructured transition metal dichalcogenide electrocatalysts for CO₂ reduction in ionic liquid. *Science* **353**, 467-470, (2016).
- 6 Schreier, M. *et al.* Solar conversion of CO₂ to CO using Earth-abundant electrocatalysts prepared by atomic layer modification of CuO. *Nat. Energy* **2**, 17087, (2017).
- 7 Cestellos-Blanco, S., Zhang, H., Kim, J. M., Shen, Y. X. & Yang, P. D. Photosynthetic semiconductor biohybrids for solar-driven biocatalysis. *Nat. Catal.* **3**, 245-255, (2020).
- 8 Yuan, H., Cheng, B., Lei, J., Jiang, L. & Han, Z. Promoting photocatalytic CO₂ reduction with a molecular copper purpurin chromophore. *Nat. Commun.* **12**, 1835, (2021).

- 9 Jiang, Z. *et al.* Filling metal-organic framework mesopores with TiO₂ for CO₂ photoreduction. *Nature* **586**, 549-554, (2020).
- 10 Xu, Y. F. *et al.* A hydrophobic FeMn@Si catalyst increases olefins from syngas by suppressing C1 by-products. *Science* **371**, 610-613, (2021).
- 11 Terrer, C. *et al.* A trade-off between plant and soil carbon storage under elevated CO₂. *Nature* **591**, 599-603, (2021).
- 12 Steffens, L. *et al.* High CO₂ levels drive the TCA cycle backwards towards autotrophy. *Nature* **592**, 784-788, (2021).
- 13 Schäppi, R. *et al.* Drop-in fuels from sunlight and air. *Nature* **601**, 63-68, (2021).
- 14 Kato, N. *et al.* A large-sized cell for solar-driven CO₂ conversion with a solar-to-formate conversion efficiency of 7.2%. *Joule* **5**, 687-705, (2021).
- 15 Wang, J. K. *et al.* 16.8% Monolithic all-perovskite triple-junction solar cells via a universal two-step solution process. *Nat. Commun.* **11**, 10, (2020).
- 16 Mi, Y. Y. *et al.* Cobalt-Iron Oxide Nanosheets for High-Efficiency Solar-Driven CO₂-H₂O Coupling Electrocatalytic Reactions. *Adv. Funct. Mater.* **30**, 2003438 (2020).
- 17 Xu, Y. *et al.* Low coordination number copper catalysts for electrochemical CO₂ methanation in a membrane electrode assembly. *Nat. Commun.* **12**, 2932-2932, (2021).
- 18 Devasia, D., Wilson, A. J., Heo, J., Mohan, V. & Jain, P. K. A rich catalog of C-C bonded species formed in CO₂ reduction on a plasmonic photocatalyst. *Nat. Commun.* **12**, 2612-2612, (2021).
- 19 Tang, C., Gong, P., Xiao, T. & Sun, Z. Direct electrosynthesis of 52% concentrated CO on silver's twin boundary. *Nat. Commun.* **12**, 2139, (2021).
- 20 Li, F. W. *et al.* Molecular tuning of CO₂-to-ethylene conversion. *Nature* **577**, 509-513, (2020).
- 21 Nam, D. H. *et al.* Molecular enhancement of heterogeneous CO₂ reduction. *Nat. Mater.* **19**, 266-276, (2020).
- 22 Ma, W. C. *et al.* Electrocatalytic reduction of CO₂ to ethylene and ethanol through hydrogen-assisted C-C coupling over fluorine-modified copper. *Nat. Catal.* **3**, 478-487, (2020).
- 23 Ma, B. *et al.* Efficient Visible-Light-Driven CO₂ Reduction by a Cobalt Molecular Catalyst Covalently Linked to Mesoporous Carbon Nitride. *J. Am. Chem. Soc.* **142**, 6188-6195, (2020).
- 24 Qiu, X.-F., Zhu, H.-L., Huang, J.-R., Liao, P.-Q. & Chen, X.-M. Highly Selective CO₂ Electroreduction to C₂H₄ Using a Metal-Organic Framework with Dual Active Sites. *J. Am. Chem. Soc.* **143**, 7242-7246, (2021).
- 25 Yan, C. *et al.* Coordinatively unsaturated nickel-nitrogen sites towards selective and high-rate CO₂ electroreduction. *Energy Environ. Sci.* **11**, 1204-1210, (2018).
- 26 Yang, H. B. *et al.* Atomically dispersed Ni(i) as the active site for electrochemical CO₂ reduction. *Nature Energy* **3**, 140-147, (2018).
- 27 Lee, W. H. *et al.* W@Ag dendrites as efficient and durable electrocatalyst for solar-to-CO conversion using scalable photovoltaic-electrochemical system. *Appl Catal. B: Environ.* **297**, 120427, (2021).

- 28 Xu, Y. Q., Zhang, W. F., Li, Y. G., Lu, P. F. & Wu, Z. S. A general bimetal-ion
adsorption strategy to prepare nickel single atom catalysts anchored on
graphene for efficient oxygen evolution reaction. *J. Energy Chem.* **43**, 52-57,
(2020).
- 29 Ju, T. *et al.* Dicarboxylation of alkenes, allenes and (hetero)arenes with CO₂ via
visible-light photoredox catalysis. *Nat. Catal.* **4**, 304-311, (2021).
- 30 Gu, J., Hsu, C.-S., Bai, L., Chen, H. M. & Hu, X. Atomically dispersed Fe³⁺
sites catalyze efficient CO₂ electroreduction to CO. *Science* **364**, 1091-1094,
(2019).
- 31 Salvatore, D. A. *et al.* Designing anion exchange membranes for CO₂
electrolysers. *Nat. Energy* **6**, 339-348, (2021).
- 32 Jia, J. Y. *et al.* Solar water splitting by photovoltaic-electrolysis with a solar-to-
hydrogen efficiency over 30%. *Nat. Commun.* **7**, 6, (2016).
- 33 Li, Y. *et al.* Selective light absorber-assisted single nickel atom catalysts for
ambient sunlight-driven CO₂ methanation. *Nat. Commun.* **10**, 2359, (2019).
- 34 Wang, L. *et al.* Black indium oxide a photothermal CO₂ hydrogenation catalyst.
Nat. Commun. **11**, 2432, (2020).
- 35 Chen, Y. *et al.* Cooperative catalysis coupling photo-/photothermal effect to
drive Sabatier reaction with unprecedented conversion and selectivity. *Joule* **5**,
3235-3251, (2021).
- 36 Rohling, J. H., Shen, J., Wang, C., Zhou, J. & Gu, C. E. Determination of binary
diffusion coefficients of gases using photothermal deflection technique. *Appl.*
Phys. B **87**, 355-362, (2007).
- 37 Belgodere, C. *et al.* Experimental determination of CO₂ diffusion coefficient in
aqueous solutions under pressure at room temperature via Raman spectroscopy:
impact of salinity (NaCl). *J. Raman Spec.* **46**, 1025-1032, (2015).
- 38 Jiang, X., Nie, X. W., Guo, X. W., Song, C. S. & Chen, J. G. G. Recent Advances
in Carbon Dioxide Hydrogenation to Methanol via Heterogeneous Catalysis.
Chem. Rev. **120**, 7984-8034, (2020).
- 39 Das, S. *et al.* Core-shell structured catalysts for thermocatalytic, photocatalytic,
and electrocatalytic conversion of CO₂. *Chem. Soc. Rev.* **49**, 2937-3004, (2020).
- 40 Li, Y. *et al.* General heterostructure strategy of photothermal materials for
scalable solar-heating hydrogen production without the consumption of
artificial energy. *Nat. Commun.* **13**, 776, (2022).
- 41 Yuan, D. *et al.* Coke and sintering resistant nickel atomically doped with ceria
nanosheets for highly efficient solar driven hydrogen production from
bioethanol. *Green Chem.* **24**, 2044-2050, (2022).
- 42 Bai, X. *et al.* Solar-heating thermocatalytic H₂ production from formic acid by
a MoS₂-graphene-nickel foam composite. *Green Chem.* **23**, 7630-7634, (2021).
- 43 Lourenço, A. C., Reis-Machado, A. S., Fortunato, E., Martins, R. & Mendes, M.
J. Sunlight-driven CO₂-to-fuel conversion: Exploring thermal and electrical
coupling between photovoltaic and electrochemical systems for optimum solar-
methane production. *Materials Today Energy* **17**, 100425, (2020).
- 44 White, J. L., Herb, J. T., Kaczur, J. J., Majsztrik, P. W. & Bocarsly, A. B. Photons

- to formate: Efficient electrochemical solar energy conversion via reduction of carbon dioxide. *J. CO₂ Util.* **7**, 1-5, (2014).
- 45 Chae, S. Y. *et al.* A perspective on practical solar to carbon monoxide production devices with economic evaluation. *Sustain. Energy Fuels* **4**, 199-212, (2020).
- 46 Urbain, F. *et al.* A prototype reactor for highly selective solar-driven CO₂ reduction to synthesis gas using nanosized earth-abundant catalysts and silicon photovoltaics. *Energy Environ. Sci.* **10**, 2256-2266, (2017).
- 47 Cheng, W.-H. *et al.* CO₂ Reduction to CO with 19% Efficiency in a Solar-Driven Gas Diffusion Electrode Flow Cell under Outdoor Solar Illumination. *ACS Energy Lett.* **5**, 470-476, (2020).

Acknowledgements

This work was supported by the Hebei Natural Science Foundation (Grant No. B2021201074), the Hebei Provincial Department of Science and Technology (Grant No. 216Z4303G), Hebei Education Department (Grant No. BJ2019016), the Advanced Talents Incubation Program of Hebei University (Grant Nos. 521000981248 and 8012605), the National Nature Science Foundation of China (Grant Nos. 51421002, 51702078, 61774053, 61504036, 51972094, and 51971157), the Natural Science Foundation of Hebei Province (Grant Nos. B2021201034, F2019201446, and F2018201058), the National Key Research and Development Program of China (2018YFB1500503-02), the Scientific Research Foundation of Hebei Agricultural University (YJ201939). Thank you for the TEM technical support provided by the Microanalysis Center, College of Physics Science and Technology, Hebei University.

Author contributions

Y. Li, L. Gu, S. wang and Q. Meng conceived the project and contributed to the design of the experiments and analysis of the data. Q. Meng proposed the system coupling idea; Y. Li provided the solar heating system strategy. X. Bai and D. Yuan performed the TiC/Cu based device preparation and characterizations. X. Bai, and F. Meng performed the catalyst preparation and characterizations. B. Liang and G. Fu provided the optical advice. F. Meng and X. San conducted the SEM and TEM examinations. Y. Li and Q. Meng wrote the paper. All the authors discussed the results and commented on the manuscript.

Additional information

Supplementary Information accompanies this paper

Competing interests: The authors declare no competing financial interests.

Reprints and permission information is available online

Publisher's note: Springer Nature remains neutral with regard to jurisdictional claims in published maps and institutional affiliations